Int. J. Electrochem. Sci., 7 **(2012)** 7325 - 7348

International Journal of ELECTROCHEMICAL SCIENCE
www.electrochemsci.org

Electrochemical Behaviour of Isopoly- and Heteropolyoxomolybdates Formed During Anodic Oxidation of Molybdenum in Seawater

Justyna Jońca[1,*], *Carole Barus*[1], *William Giraud*[1], *Danièle Thouron*[1], *Véronique Garçon*[1], *Maurice Comtat*[2]

[1] Laboratoire d'Etudes en Géophysique et Océanographie Spatiales, UMR 5566, 18 Avenue Edouard Belin, 31401 Toulouse Cedex 9, France
[2] Laboratoire de Génie Chimique, UMR 5503, Université Paul Sabatier, 118 Route de Narbonne, 31062 Toulouse Cedex, France
[*]E-mail: justyna.jonca@legos.obs-mip.fr

Received: 1 March 2012 / *Accepted:* 3 July 2012 / *Published:* 1 August 2012

The electrochemical behaviour of isopoly- and heteropolyoxomolybdates formed during anodic oxidation of molybdenum in seawater at constant current intensity was investigated in this work. The results supported by spectrophotometry clearly indicate the formation of mixed valence molybdates (V/VI) during this process. The electrochemical behaviour of isopolyoxomolybdates shows a typical quasi-reversible mass-transport limited system coupled with an adsorption of reduced species and under some kinetic limitations. For heteropolyoxomolybdates a reversible mass-transport limited system coupled with an homogeneous chemical reaction was found. The coupled reaction, probably protonation, prevents a rapid heterogeneous electron transfer for heteropolyoxomolybdate complex. The phenomenon is more noticeable for the phosphomolybdate complex since the protonation step has a greater influence on the registered voltammograms. The presented results have a great importance in research areas where molybdate chemistry is used in detection of silicate and phosphate, namely in seawater.

Keywords: isopolyoxomolybdates, heteropolyoxomolybdates, molybdenum oxidation, voltammetry

1. INTRODUCTION

Polyoxomolybdates have long been applied for detection, separation and quantification, based on properties such as high molecular mass, electrochemical activity, reducibility, and variety of elements that can be incorporated. One of the most widely used application has been the spectrophotometric determination of phosphate and silicate in seawater after reduction of $[XMo_{12}O_{40}]^{n-}$

(X=Si, P) to “heteropoly blues” by ascorbic acid [1-3]. The determination of P, Si, Ge and As has been also performed by differential pulse anodic voltammetry [4], cyclic voltammetry [5, 6] and amperometry [7, 8]. Recently, a totally new electrochemical method was developed in our group for determination of silicate [9, 10] and phosphate [11] without addition of any liquid reagents. The method is based on the anodic oxidation of molybdenum in seawater in order to form silico- or phosphomolybdate complex electrochemically detectable either by means of cyclic voltammetry or amperometry. This method offers a great possibility for the *in situ* phosphate and silicate monitoring in seawater, but our knowledge about different forms of molybdates produced during molybdenum oxidation is limited. The purpose of this work is to find what kind of isopoly- and heteropolyoxomolybdates complexes are formed during electrochemical oxidation of molybdenum electrode in seawater. These results will help us to develop a first electrochemical sensor for the *in situ* detection of phosphate and silicate in the ocean and to elucidate the complex chemistry of isopoly- and heteropolyoxomolybdates.

Oxidation of molybdenum has been performed in several solutions. The polarization curve for molybdenum in acidic medium was divided in three regions: cathodic, passive and transpassive [12, 13]. In the first region hydrogen evolution proceeds on the electrode; in the middle zone a layer of MoO_2 leads to passivity; in the high potential region, the MoO_2 layer is transformed to MoO_3 and Mo dissolves to form molybdate. Bojinov et al. [14, 15] suggested that the final soluble product of the molybdenum oxidation in acid solution is Mo(VI) which can exist according to Hull [16] as molybdate or polymolybdate species (depending on pH). However, Itagaki et al. [13] claimed coexistence of Mo(V) and Mo(VI) in the solution after oxidation of molybdenum at high anodic potentials. Chukalovskaya et al. [17] stated that the final soluble product in this region was molybdenum blue. The Mo(VI)/Mo(V) ratio of molybdenum blue composition was 0.5.

The electrochemical behaviour of molybdenum in basic solutions was also investigated but to a lesser extent. However, the molybdenum electrode in this medium was covered with a film consisting mainly of $Mo(OH)_3$, MoO_2 and MoO_3 [16]. The soluble product of anodic oxidation at higher potentials (0.2 – 1.0 V) was Mo(VI) as monomeric MoO_4^{2-} species since the pH was basic. Moreover some Mo(III) species were reported but at much lower concentrations than when oxidizing molybdenum at low potentials (-0.3V – 0.2 V). At very high potentials > 1.0 V the molybdate (V) species were also found in the solution.

There are only a few publications about the oxidation of molybdenum in neutral medium like seawater [10] or 0.15 mol L^{-1} NaCl solution [18]. Wang et al. [18] stated that molybdate oxides film consists of MoO_2 and Mo_2O_3, but the final soluble product is Mo(VI). Lacombe et al. [10] supposed also that the produced soluble Mo(VI) can exist in different forms depending on the pH of the solution.

It is worth noticing also that the produced anodic layers of molybdenum oxides were conductive [19]. This is very important for our purposes since the molybdenum electrode could not be cleaned *in situ* after oxidation.

As it was mentioned above, polyoxomolybdate form depends strongly on pH and concentration. It was found that, at very low concentrations ($<10^{-4}$ mol L^{-1}), mononuclear species predominate. At higher concentrations ($>10^{-3}$ mol L^{-1}), the polynuclear species appear [20]. Additionally, it was found that in the pH 7-12 the main species is MoO_4^{2-} and its protonated forms:

$HMoO_4^-$ and H_2MoO_4, but at pH 3-5 the $Mo_7O_{24}^{6-}$, $HMo_7O_{24}^{5-}$, $H_2Mo_7O_{24}^{4-}$, $H_3Mo_7O_{24}^{3-}$ are predominant. Finally at pH 2 and below, the $Mo_8O_{26}^{4-}$ [21] appears and $[Mo_{36}O_{112}(H_2O)_{16}]^{8-}$ was also found [22]. Future acidification might lead to more and more complicated polyoxomolybdates due to a polymerization process. In the aqueous solutions lower oxidation state molybdates are not very well defined. The aqua ions of Mo(V) and Mo(IV) are $[Mo_2O_4]^{2+}$ and $[Mo_3O_4]^{4+}$. The aqueous chemistry of Mo(III) suggests monomeric $MoO(H_2O)_5^+$ or $Mo(H_2O)_6^{3+}$ and dimer $[(H_2O)_5Mo\text{-}O\text{-}Mo(H_2O)_5]^{4+}$ [21, 23].

Polyoxomolybdates can incorporate other ions into their structure, forming heteropolyoxomolybdates. The major silicomolybdate is $SiMo_{12}O_{40}^{4-}$. The α– and β– isomers are known, but the α– isomer is more stable. Both appear in acidic medium, but the first one corresponds to a pH range about 3.5-4.5, the second one to a pH about 0.8-2.5 [24]. In pH higher than 4 the $SiMo_{11}O_{40}^{4-}$ is formed but upon simple acidification or excess of MoO_4^{2-} the $SiMo_{12}O_{40}^{4-}$ form is predominant [25]. The major phosphomolybdate are α– and β– $PMo_{12}O_{40}^{3-}$, $P_2Mo_{18}O_{62}^{6-}$, $PMo_{11}O_{37}^{3-}$, $PMo_{10}O_{34}^{3-}$, $PMo_9O_{31}(OH_2)_3^{3-}$, $P_2Mo_5O_{23}^{6-}$ [26]. The Keggin anion $PMo_{12}O_{40}^{3-}$ is the most known complex of phosphomolybdates which appears in very acidic aqueous solutions. The β– isomer as any β– Keggin anion is less stable in aqueus solutions than the α– one [25].

The study of molybdate complexes in this work was performed by electrochemistry, spectrophotometry and equilibrium analysis. It is a first paper describing in details the electrochemical behavior of isopoly- and heteropolyoxomolybdates formed during molybdenum oxidation in seawater.

2. REAGENTS AND SOLUTIONS

Molybdate solution (1 mol L^{-1}) was prepared by dilution of 2.42 g of sodium molybdate (VI) (Merck) in 10 mL of milliQ water.

Sulphuric acid solutions (0.5 mol L^{-1} and 5 mol L^{-1}) were prepared by dilution of concentrated sulphuric acid (Merck) in milliQ water.

Phosphate and silicate solutions were prepared with sodium silicofluoride (Na_2SiF_6, Merck) and potassium dihydrogen phosphate (KH_2PO_4, Merck).

The ascorbic acid for spectrophotometrical analysis was prepared by dissolution of 7.5 g of ascorbic acid (Sigma) in 250 mL milliQ water.

All experiments were performed in artificial sea water at salinity 35.4.

3. METHODS

3.1. Electrochemistry

The reference electrode was an Ag/AgCl/3 mol L^{-1} KCl electrode (Metrohm). All the following potentials are given relative to this electrode. Electrochemical measurements were carried out with a potentiostat μ-Autolab III (Metrohm).

Voltammograms at a stationary or rotating disk electrode were recorded in a three electrode cell with a platinum counter electrode. Working electrode was in gold (Metrohm, area 0.07 cm^2). The electrode was polished with lapping film sheet (3 mol L^{-1} Aluminium Oxide, 1 µm) and electrochemically cleaned in 0.5 mol L^{-1} sulphuric acid solution (5 scans, from 0.0 to 1.5 V, 200 mV s^{-1}) before each measurement.

The molybdenum electrode (Good Fellow Metals, purity: 99.9%) has an area of 0.20 cm^2 (or $7.85*10^{-3}$ cm^2). The intensity potential curves for molybdenum oxidation were obtained with small electrode ($7.85*10^{-3}$ cm^2). The oxidation of molybdenum at constant current was done with a bigger one (0.20 cm^2).

The production of isopoly- and heteropolyoxomolybdates without addition of any liquid reagents in our conditions is based on the use of a 20 mL cell divided in two by a membrane (N117 DuPont^{TM} Nafion^{R} PFSA Membranes); the first part of the cell was filled with 3 mL of the solution, the second with 17 mL of solution. Molybdenum, reference and working electrodes were in the anodic compartment while the counter electrode was in the cathodic one. Molybdates were produced by molybdenum anodic oxidation performed in artificial seawater at a constant current electrolysis (50 mA) during different times.

3.2. Spectrophotometry

The measurements were carried out on a UV-Vis spectrophotometer (Varian Inc. Cary 50, Australia) using 10 mm 100-QS quartz cuve (Hellma Analytics, Germany). The spectrograms for isopoly- and heteropolyoxomolybdates were registered at different pH and concentrations of molybdate. The final solution was treated with ascorbic acid to reduce heteropolyoxomolybdates (VI) to molybdenum blue which gives a spectrum in visible (400-900 nm). Spectrograms for isopoly- and heteropolyoxomolybdates created without addition of any liquid reagents were performed after different oxidation times of the molybdenum electrode in artificial seawater. The spectrograms (400-900 nm) were registered in presence and absence of ascorbic acid.

3.3. Equilibrium analysis

Artificial sea water solutions at different initial pH were prepared and the 1 mol L^{-1} molybdate solution was added to obtain different final concentrations. The pH was measured before and after addition of molybdate.

The pH was also measured after different times of the molybdenum electrode oxidation and the concentration of protons was compared with theoretical values obtained from Faraday’s law.

The pH was controlled using the pH meter Metrohm 744.

4. RESULTS AND DISCUSSION

4.1. Molybdenum oxidation

Molybdate and protons were produced by anodic oxidation of molybdenum in the electrochemical cell according to reaction (1). By separation of the anode from the cathode with a

Nafion diaphragm, we eliminate the consumption of the protons on the platinum cathode. This allows us to achieve the desired pH in the anodic compartment.

$$Mo + 4H_2O \rightarrow MoO_4^{2-} + 8\ H^+ + 6e^- \qquad (1)$$

The intensity potential curves for molybdate oxidation in natural seawater at different pH and in 0.6 mol L^{-1} NaCl solution are presented on Fig. 1a. The anodic parts of the Tafel plots (Fig. 1b) can be described by a general equation (2).

$$\eta = \frac{2.3RT}{\alpha F}\log j_0 - \frac{2.3RT}{\alpha F}\log j \qquad (2)$$

Where j is the current density (A cm^{-2}), j_0 is the exchange current density (A cm^{-2}), α is the anodic transfer coefficient, η is the overpotential (V), F is the Faraday constant (C mol^{-1}) and R is the molar gas constant (J mol^{-1} K^{-1}).

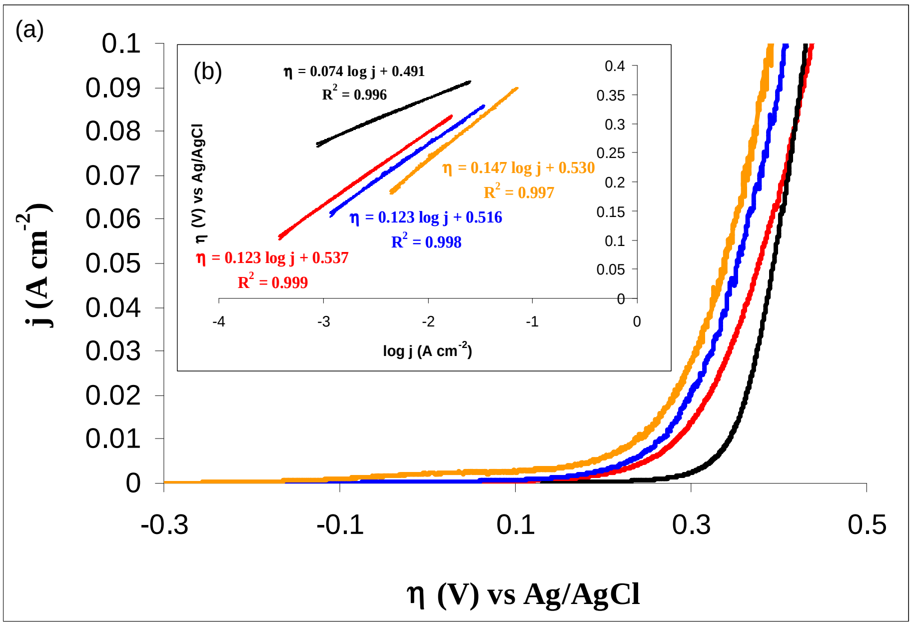

Figure 1. (a) Linear sweep voltammograms (5 mV s^{-1}) for molybdenum oxidation in 0.6 mol L^{-1} NaCl solution (red line) and in natural seawater at pH 7.8 (blue line), pH 1.0 (black line) and pH 10 (orange line); (b) corresponding Tafel plots.

The Tafel plot slopes in 0.6 mol L^{-1} NaCl and in natural seawater (pH 7.8) are the same and equal to 0.123. The exchange current density was $10^{-4.1}$ A cm^{-2} for seawater and $10^{-4.3}$ A cm^{-2} for the NaCl solution. The determined transfer coefficient α from equation (2) was equal to about 0.46 for both media. Acidification of seawater to pH 1.0 by sulphuric acid caused a decrease of the Tafel plot slope to 0.074 and the exchange current density is decreasing to $10^{-6.7}$ A cm^{-2}. The alkalinisation of seawater with sodium hydroxide to pH 10 results in the increase of the Tafel plot slope to 0.147 and an increase of exchange current density to $10^{-3.6}$ A cm^{-2}. The transfer coefficient was 0.39 for seawater at pH 10 and 0.79 for seawater at pH 1.0. The obtained results showed similar order of magnitude that those obtained by Wang et al. [18] in different solutions and clearly indicate that the passivation of molybdenum can be achieved more easily in acidic medium than in basic one. The following experiments may be done in artificial seawater because the electrochemical behaviour of molybdenum electrode in 0.6 mol L^{-1} NaCl solution is very similar to the one in natural seawater (pH 7.8).

For further analysis a constant current intensity is chosen for the molybdenum oxidation in order to control the quantity of molybdate formed, according to the Faraday's law. We chose a current of 50 mA corresponding to potentials between 0.8 – 1.0 V and thus, we are in the transpassive region where active dissolution of molybdenum to molybdate occurs.

The concentration of molybdate and protons increases with oxidation time. A longer oxidation time of molybdenum leads to a higher molybdate concentration in the solution and the percentage of polynuclear species increases.

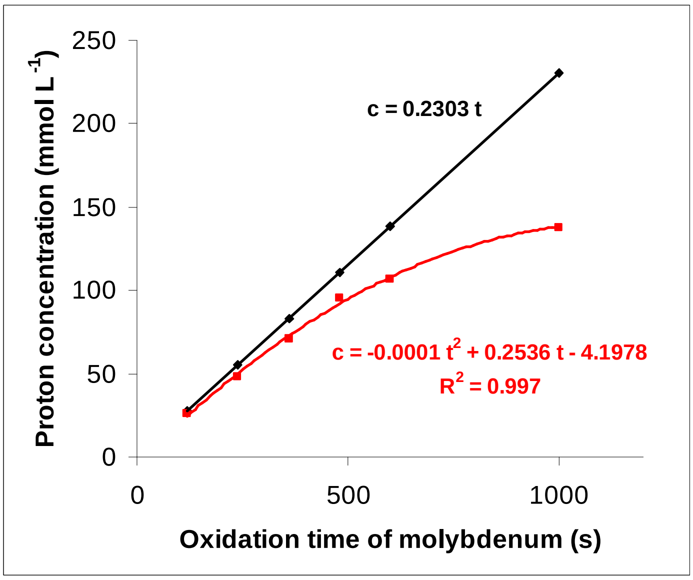

Figure 2. Comparison of (black line) expected value of proton concentration (calculated from Faraday's law) with (red line) experimental measurements of pH.

Besides, the formation of polyoxomolybdates consumes some protons and more and more complex polyoxomolybdates are created with an increase of acidification. Having all this in mind, we assume that equation (1) will change with time during the molybdenum oxidation. Fig. 2 presents the comparison between the expected value of protons and that calculated from measured pH after different oxidation times. The results show that the measured concentration of protons is lower than the theoretical one. This may be due to mentioned protonation process of molybdates. Some protons are used for the formation of polyoxomolybdates and thus the measured pH for the solution is higher than expected.

In spite of the complexity of the reactions occurring during the molybdenum dissolution, the measured pH in the solution is repeatable with a precision of 1.7% for 500s of oxidation [11]. The colour of the solution after molybdenum dissolution is blue and its intensity increases with time of oxidation. This fact clearly indicates the presence of isopolyoxomolybdate complexes containing Mo(V) and Mo(VI) known as molybdenum blues. Moreover, the blue colour appears in both 0.6 mol L^{-1} NaCl solutions: in presence and absence of phosphate (or silicate). Additionally, the surface of the oxidized molybdenum electrode is covered with a dark blue oxide layer which is conductive as it had been noticed before [19].

4.2. Electrochemical behavior of isopolyoxomolybdates

4.2.1.Cyclic voltammetry

Cyclic voltammetry was performed on a 3 mm gold disk electrode (200 mV s^{-1}) after each oxidation time of molybdenum in 0.6 mol L^{-1} NaCl solution and presented on Fig. 3a. For comparison cyclic voltammograms made with isopolyoxomolybdates created by addition of sodium molybdate (VI) and sulphuric acid are presented on Fig. 3b where the value of molybdate concentration and pH were the same as those achieved during the oxidation of molybdenum. For clarity only selected curves are presented.

Cyclic voltammetry of isopolyoxomolybdates created by addition of sodium molybdate (VI) to an acidified solution was investigated before by Krishnan et al. [21]. The work shows clearly that the shape of the curves depends strongly on pH since different molybdate species might be formed from simple MoO_4^{2-} to protonated species of $Mo_8O_{26}^{4-}$. Similar conclusions were made in this work but the situation is even more delicate since the pH of medium was lower (pH 1-2) and diverse isopolyoxomolybdates can be formed as it is suggested by different shapes of voltammograms. Calculation of parameter “z” –the number of protons consumed by one molecule of MoO_4^{2-} is a proper equilibrium method to indicate the isopolyoxomolybdates formed at different conditions (Table 1.). The method is based on pH measurements of an acidified solution before and after addition of sodium molybdate at adequate concentration. The difference in proton concentrations is divided by the molybdate concentration giving a value of parameter “z” characteristic for each created molybdate species. Moreover, total formation reaction can be proposed for each species (equations 3a-e). It is clear from these results that with growing acidification and molybdate concentration more and more complicated isopolyoxomolybdates are formed due to protonation and condensation reactions. The proposed forms of isopolyoxomolybdates are in good agreement with a reaction model of the equilibrium system for molybdate described by Cruywagen et al. [27].

$$8\ MoO_4^{2-} + 12\ H^+ \rightarrow Mo_8O_{26}^{4-} + 6\ H_2O \qquad (3a)$$

$$13\ MoO_4^{2-} + 22\ H^+ \rightarrow H_2Mo_{13}O_{42}^{4-} + 10\ H_2O \qquad (3b)$$

$$13\ MoO_4^{2-} + 21\ H^+ \rightarrow HMo_{13}O_{42}^{5-} + 10\ H_2O \qquad (3c)$$

$$12\ MoO_4^{2-} + 17\ H^+ \rightarrow HMo_{12}O_{40}^{7-} + 8\ H_2O \tag{3d}$$

$$36\ MoO_4^{2-} + 65\ H^+ \rightarrow HMo_{36}O_{112}^{7-} + 32\ H_2O \tag{3e}$$

The cyclic voltammetry for isopolyoxomolybdates formed during oxidation of molybdenum differs from the characteristics described above. The shapes of the curves registered after each oxidation times are similar to each other, the signal peak is more or less at the same potential and the reduction peak current density is proportional to the molybdate concentration calculated from Faraday's law (j_{pc}=-0.323c-0.664, R^2=0.995). These results suggest that during the oxidation of molybdenum in seawater only one species of molybdate is formed and it is rather different than those achieved during simple addition of sulphuric acid and sodium molybdate (VI). However, it is not possible at this step to propose a chemical formula for this species.

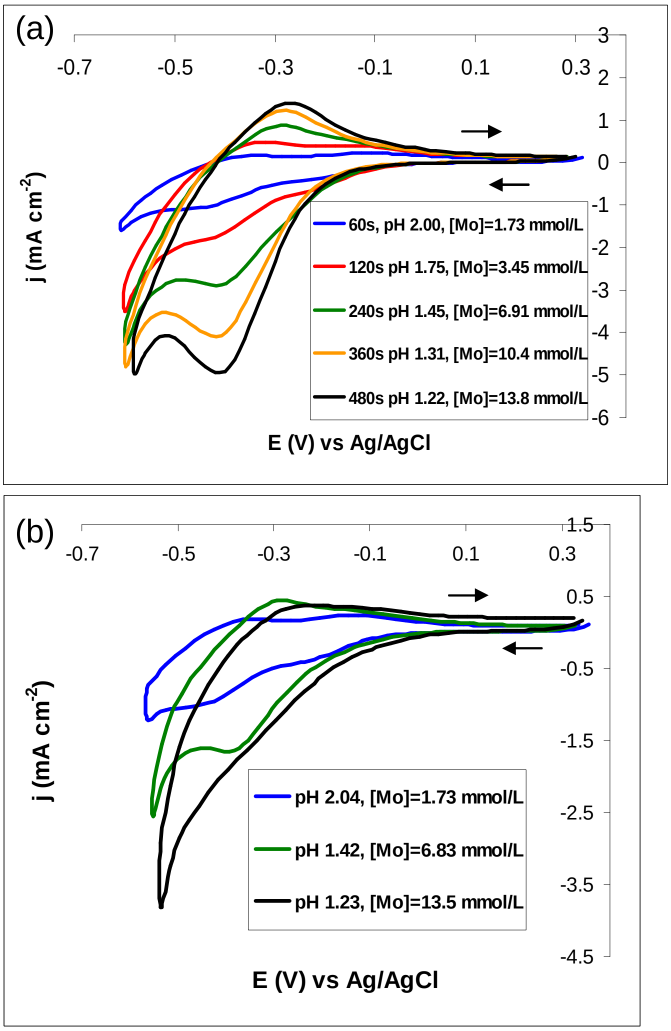

Figure 3. Cyclic voltammograms recorded on a gold disk electrode (3 mm, 200 mV s^{-1}) for isopolyoxomolybdates created by: (a) oxidation of molybdenum at constant current of 50 mA in 0.6 mol L^{-1} NaCl solution at several times; (b) simple addition of sulphuric acid and sodium molybdate (VI) to 0.6 mol L^{-1} NaCl solution to achieve appropriate pH and molybdate concentrations.

Table 1. Parameter « z » - the number of protons consumed by one molecule of MoO_4^{2-} calculated for different pH and molybdate concentrations with some proposition of chemical formula for the created isopolyoxomolybdates.

$[MoO_4^{2-}]$ (mmol L^{-1})	Initial pH*	Final pH**	Parameter « z »	Proposed form of isopolyoxomolybdate	Eq.
1.73	1.93	2.04	1.52 (σ=0.021)	$Mo_8O_{26}^{4-}$ (8, 12)	3a
3.45	1.65	1.78	1.69 (σ=0.015)	$H_2Mo_{13}O_{42}^{4-}$ (13, 22)	3b
6.91	1.31	1.42	1.61 (σ=0.014)	$HMo_{13}O_{42}^{5-}$ (13, 21)	3c
10.0	1.21	1.32	1.40 (σ=0.017)	$HMo_{12}O_{40}^{7-}$ (12, 17)	3d
13.8	1.08	1.23	1.80 (σ=0.007)	$HMo_{36}O_{112}^{7-}$ (36, 65)	3e
17.3	0.87	0.98	1.80 (σ=0.010)	$HMo_{36}O_{112}^{7-}$ (36, 65)	3e

* pH of acidified NaCl solution before addition of molybdate
** pH of acidified NaCl solution after addition of molybdate
σ-standard deviation

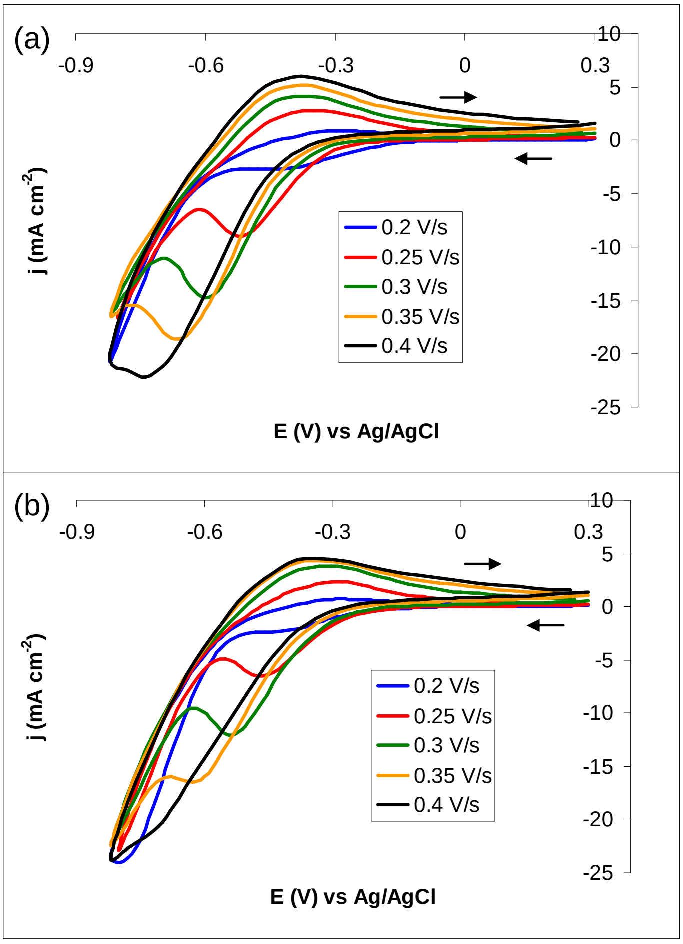

Figure 4. Cyclic voltammograms recorded on a gold disk electrode (3 mm) at different scan rates for isopolyoxomolybdates created by: (a) oxidation of molybdenum in 0.6 mol L^{-1} NaCl solution during 240 s at constant current of 50 mA (pH 1.45, [Mo]=6.91 mmol L^{-1}); (b) simple addition of sulphuric acid and sodium molybdate (VI) to 0.6 mol L^{-1} NaCl solution (pH 1.42, [Mo]=6.83 mmol L^{-1}).

In spite of many differences between isopolyoxomolybdates formed during molybdenum oxidation and by simple addition of sodium molybdate (VI) to sulphuric acid solution, the cyclic voltammograms show some similarities. In both methods, the reduction current density (j_{pc}) is proportional to the square root of the scan rate (Fig. 4), as it is indicated by equations: j_{pc}=-105.3 $\upsilon^{-1/2}$+ 45.5; R^2=0.993 (isopolyoxomolybdates created by simple addition of reagents), j_{pc}=-106.5 $\upsilon^{-1/2}$+ 44.5; R^2=0.992 (isopolyoxomolybdates created by molybdenum oxidation). However, the reverse oxidation peaks (j_{pa}) are less pronounced (the ratio j_{pa} over j_{pc} is smaller than 1) which is indicative of a very slow rate of electron transfer. Reduction potential peak (E_{pc}) shifts to higher potentials as scan rate (υ) increases as it is indicated by equations: E_{pc}=-1.34 υ-0.141; R^2=0.992 (isopolyoxomolybdates created by simple addition of reagents), E_{pc}=-1.62υ-0.10; R^2=0.983 (isopolyoxomolybdates created by molybdenum oxidation). Moreover, the peaks are broader and the peak separation (E_{pa}-E_{pc}) increases with scan rate (υ) as described by equations: (E_{pa}-E_{pc})=0.902υ-0.054; R^2=0.985 (isopolyoxomolybdates created by simple addition of reagents), (E_{pa}-E_{pc})=1.19υ-0.137; R^2=0.985 (isopolyoxomolybdates created by molybdenum oxidation). These results indicate a typical quasi-reversible mass-transfer limited process.

4.2.2. Linear sweep voltammetry

Measurements were performed on a 3mm rotating disk gold electrode (1000 rpm, 5 mV s^{-1}) after each oxidation time of molybdenum in 0.6 mol L^{-1} NaCl solution and presented on Fig. 5a. For comparison a linear sweep voltammetry made for isopolyoxomolybdates created by addition of molybdate and sulphuric acid is presented on Fig. 5b where the value of molybdate concentration and pH were the same as those achieved during oxidation of molybdenum. For clarity only selected curves are presented.

The comparison of both conditions showed some similarities. After experiments, the surface of the gold electrode was covered with a thin dark layer. It has been noticed before by Kuznestov et al. [28] for isopolyoxomolybdates created by simple addition of acid to molybdate (VI) ions. He stated that the thin layer consists of compounds of Mo of lower valences. The reduced solution becomes blue after reduction of isopolyoxomolybdates created by simple addition of sulphuric acid and sodium molybdate which indicates the presence of mixed valence (VI/V) molybdates. Similar results could not be observed for isopolyoxomolybdates created by oxidation of molybdenum since the solution after this process was already blue.

For both methods, the voltammograms presented on Fig. 5 show two waves. The wave at less negative potentials which becomes a peak at higher molybdate concentrations is characteristic of an electrochemical process coupled with adsorption of reduced species or coupled with a homogenous reaction. Additionally, the limiting current density (j_{lim}) for this wave is independent on rotation rate (ω) as it is shown on Fig. 6. These results might suggest that the wave indicates a process with adsorption of the reduced species.

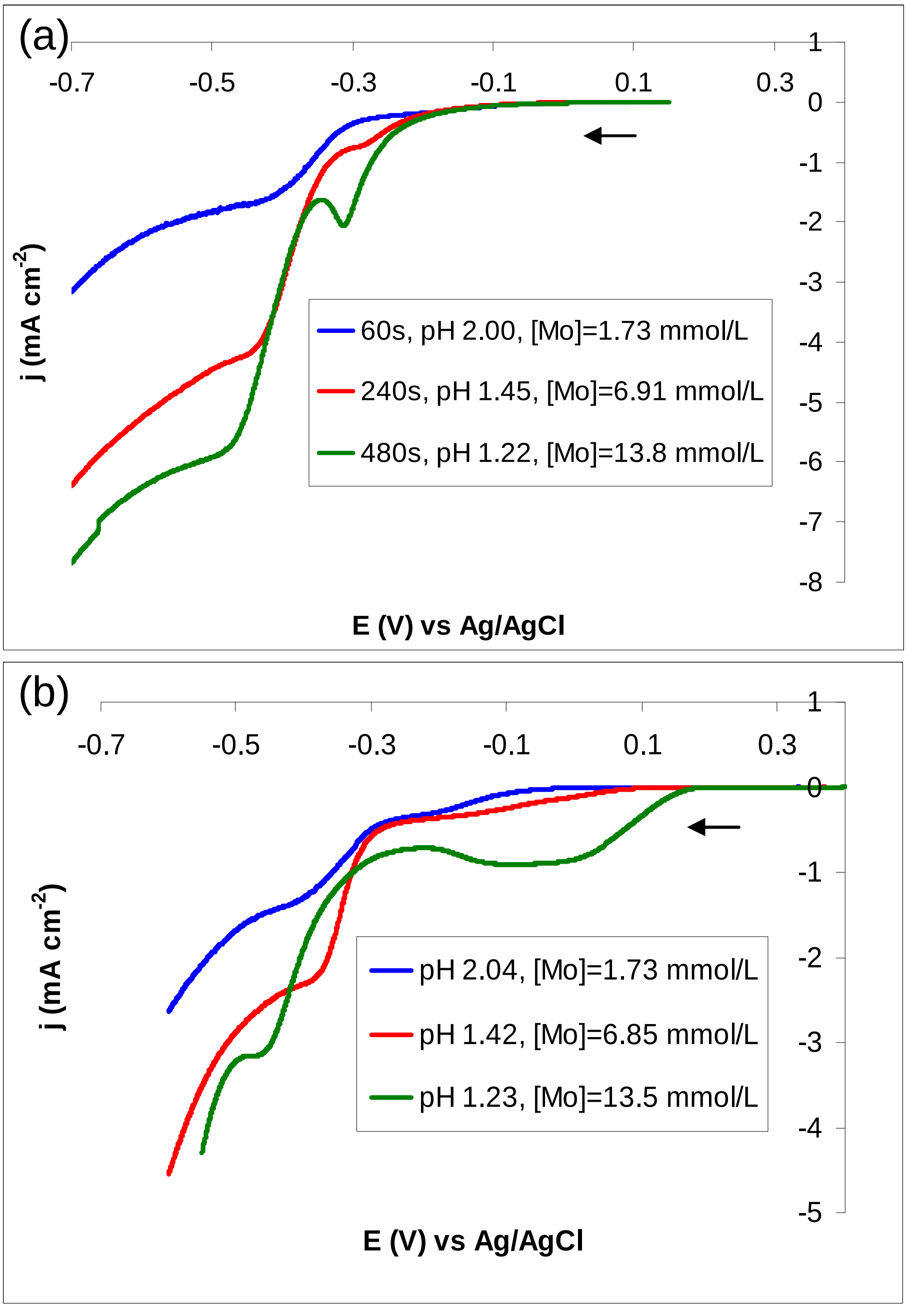

Figure 5. Linear sweep voltammograms recorded on a rotating gold disk electrode (3 mm, 1000 rpm, 5 mV s^{-1}) for isopolyoxomolybdates created by: (a) oxidation of molybdenum at constant current of 50 mA in 0.6 mol L^{-1} NaCl solution at several times; (b) simple addition of sulphuric acid and sodium molybdate (VI) to 0.6 mol L^{-1} NaCl solution to achieve appropriate pH and molybdate concentrations.

The second wave occurring at more negative potentials is more dependent on the rotation rate. However, for the greater rotation rates (up to 3000 rpm) the limiting current density (j_{lim}) becomes constant. A deviation of a plot $j_{lim}=f(\omega^{1/2})$ from a straight line intersecting the origin suggests that a kinetic limitation is involved in the electron-transfer reaction [29]. In this case, one can measure the limiting current density in the absence of any mass transport effects (j_k). There is a well-defined point where the limiting current density starts to be kinetically limited (Fig. 7).

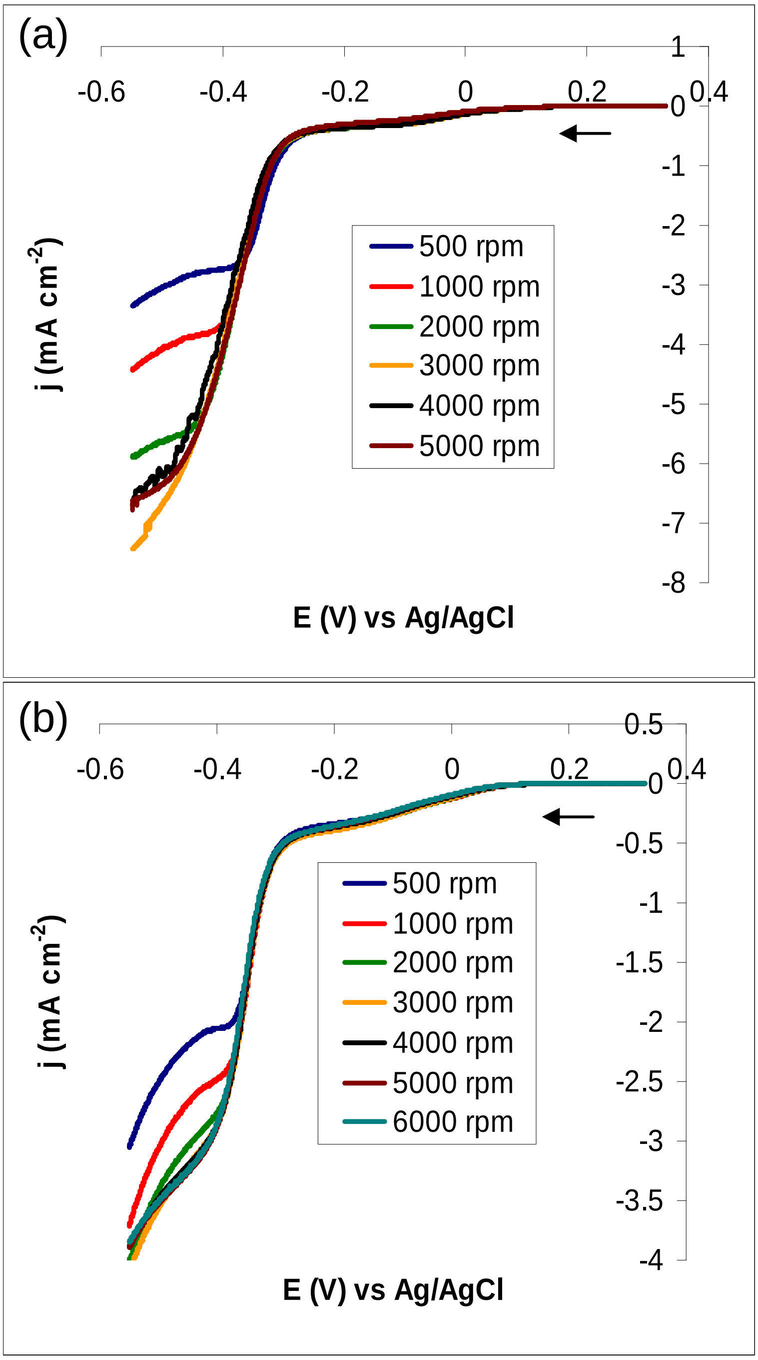

Figure 6. Linear sweep voltammograms recorded on a rotating gold disk electrode (3 mm, 5 mV s^{-1}) at different rotation rates for isopolyoxomolybdates created by: (a) oxidation of molybdenum in 0.6 mol L^{-1} NaCl solution during 240 s at constant current of 50 mA (pH 1.45, [Mo]=6.91 mmol L^{-1}); (b) simple addition of sulphuric acid and sodium molybdate (VI) to 0.6 mol L^{-1} NaCl (pH 1.42, [Mo]=6.83 mmol L^{-1}).

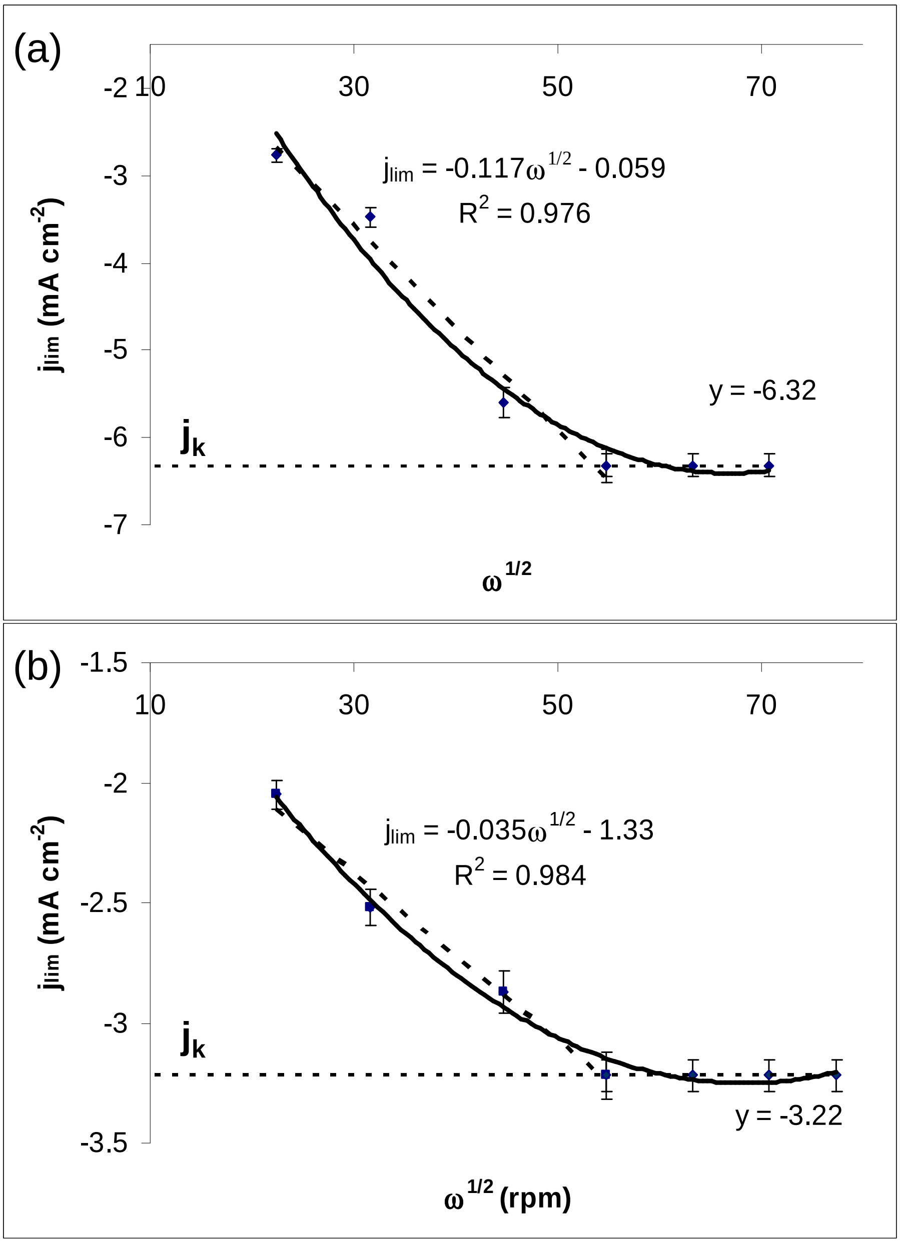

Figure 7. Limiting current density vs. square root of the electrode rotation rate for isopolyoxomolybdates created by: (a) oxidation of molybdenum in 0.6 mol L^{-1} NaCl solution during 240 s at constant current of 50 mA (pH 1.45, [Mo] =6.91 mmol L^{-1}); (b) simple addition of sulphuric acid and sodium molybdate (VI) to 0.6 mol L^{-1} NaCl (pH 1.42, [Mo] =6.83 mmol L^{-1}).

Thus, the j_k for isopolyoxomolybdates created by addition of liquid reagents is equal to -3.22 mA cm^{-2}, whereas for isopolyoxomolybdates created by oxidation of molybdenum is equal to about -6.32 mA cm^{-2}. This allows to calculate the heterogeneous rate constant (k_f) due to equation (4):

$$k_f = \frac{j_k}{FAC_0^*} \qquad (4)$$

Where F is the Faraday's constant (C mol^{-1}), A is the electrode surface (cm^2), C_0^* is the concentration of reduced species (mol cm^{-3}), k_f is the heterogeneous rate constant (cm s^{-1}), j_k is the kinetically limited current density (A cm^{-2}).

The calculated heterogeneous rate constant is equal to 4.7 * 10^{-3} cm s^{-1} (for isopolyoxomolybdates created by addition of liquid reagents) and 9.3 * 10^{-3} cm s^{-1} (for isopolyoxomolybdates created by oxidation of molybdenum).

When comparing both methods, some differences indicate the formation of more complicated species during molybdenum oxidation, than in the conditions were isopolyoxomolybdates are created by simple addition of acid to molybdate (VI) solution. For instance the potentials of the waves on Fig. 5a are shifted to more negative values than those corresponding to Fig. 5b.

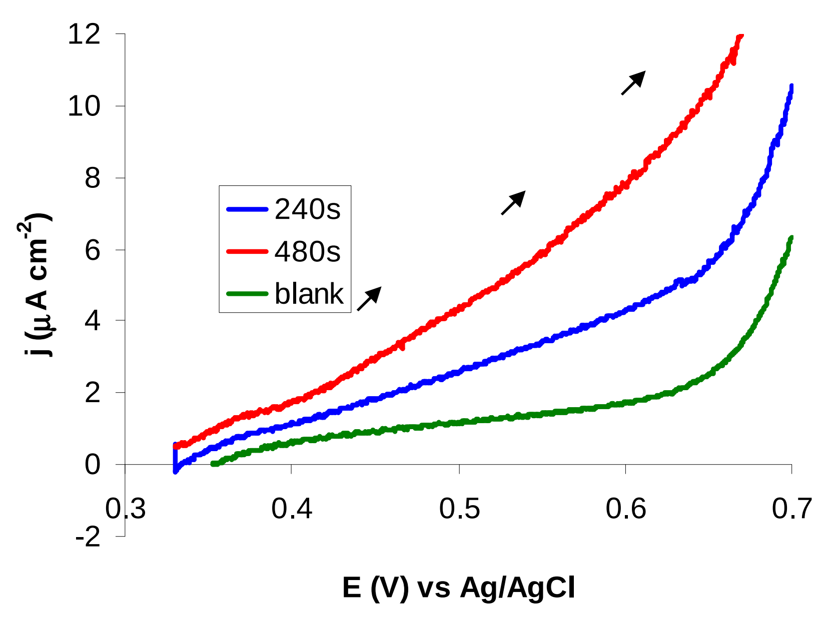

Figure 8. Linear sweep voltammograms recorded on a rotating gold disk electrode (3 mm, 5 mV s^{-1}, 1000 rpm) for isopolyoxomolybdates created by oxidation of molybdenum in 0.6 mol L^{-1} NaCl solution during 240s and 480s at constant current of 50 mA.

It was mentioned above that isopolyoxomolybdates containing Mo(V) and Mo(VI) can be formed during molybdenum oxidation. A linear sweep voltammetry was performed on a gold electrode (1000 rpm, 5 mV s^{-1}) after molybdenum oxidation in order to find molybdates at lower valences. The presence of a wave at more positive potentials than +0.3 V (Fig. 8) clearly indicates the presence of Mo (V) in the solution. Moreover, spectrophotometry in visible was performed after oxidation of molybdenum and presented on Fig. 9. The data showed peaks at wavelengths corresponding to molybdenum blue spectrum with a maximum at 800 nm. This kind of spectrum did not appear when only Mo (VI) is present in the solution.

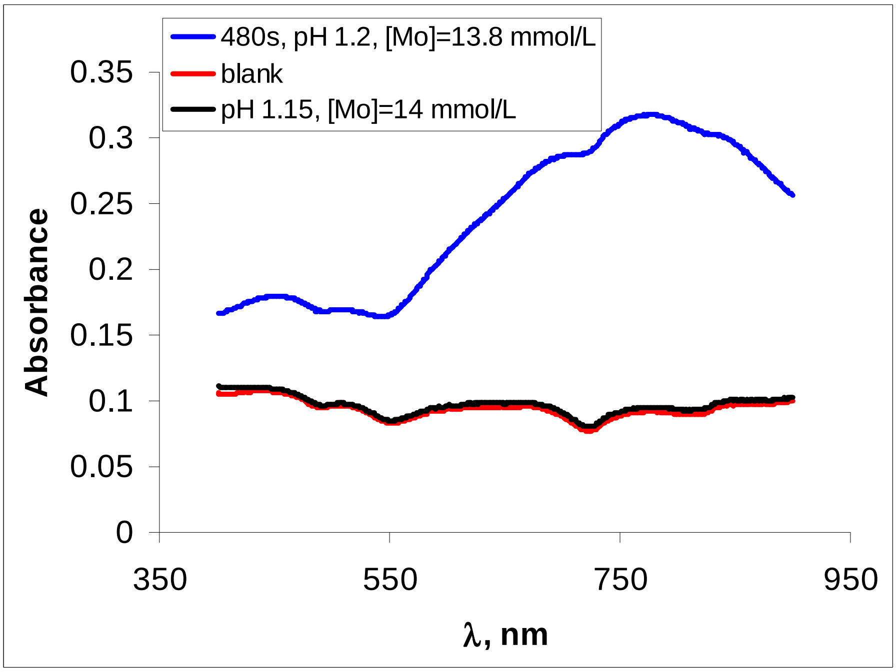

Figure 9. Absorbance as a function of wavelength for isopolyoxomolybdates created by: (black line) simple addition of sulphuric acid and sodium molybdate (VI) to 0.6 mol L^{-1} NaCl; (blue line) oxidation of molybdenum in 0.6 mol L^{-1} NaCl solution during 480 s at constant current of 50 mA.

4.3. Electrochemical behaviour of heteropolyoxomolybdates

4.3.1. Cyclic voltammetry

Cyclic voltammetry for hereropolyoxomolybdates was performed on a 3 mm disk gold electrode (50 mV s^{-1}) after oxidation of molybdenum in 0.6 mol L^{-1} NaCl solution containing phosphate or silicate at a concentration of about 100 μmol L^{-1}. For comparison, a cyclic voltammetry was made for heteropolyoxomolybdates created by addition of sodium molybdate (VI) and sulphuric acid to the 0.6 mol L^{-1} NaCl solution containing phosphate or silicate at a concentration of about 100 μmol L^{-1}, where the value of molybdate concentration and pH were the same as those achieved during oxidation of molybdenum. The resulting voltammograms are presented on Fig. 10 and show four peaks: two oxidation and two reduction ones. The reduction peaks are at 0.32 V and 0.45 V for phosphomolybdate complex and at 0.26 V and 0.37 V for silicomolybdate one. The oxidation peaks are at 0.40 V, 0.53 V and 0.32 V, 0.43 V, respectively.

Comparison of both conditions shows a great agreement between voltammograms for heteropolyoxomolybdates created by oxidation of molybdenum and by simple addition of sulphuric acid and sodium molybdate (VI) to the sample containing phosphate or silicate. This suggests that the formed types of heteropolyoxomolybdates are the same. However, the voltammograms for phosphomolybdate species differ from that of the silicomolybdate complex in several ways. The peaks are broader and not as well defined. The peaks separation (E_{pa}-E_{pc}) is bigger on phosphomolybdate voltamograms (80 mV) than for silicomolybdate ones (60 mV). The peak currents densities for the phosphomolybdate complex are lower than for the silicomolybdate one. These results clearly indicate that the electrode reactions are limited by a homogeneous chemical step which prevents rapid electron transfer for phosphomolybdate complex. It was concluded by Carpenter et al. [15] that the electrode reactions of both phosphomolybdate and silicomolybdate complexes are preceded by a pH dependent chemical reaction, probably protonation. This chemical step is faster for the silicomolybdate than for phosphomolybdate complex (equation 6) and thus has a small influence on the registered voltammograms.

$$SiMo_{12}O_{40}^{4-} + H^{+} \leftrightarrow HSiMo_{12}O_{40}^{3-} \qquad (6)$$

The change in pH or molybdate concentration does not influence the potential or shape peak, but it has a strong influence on peak current density for both silicomolybdate and phosphomolybdate complexes. Thus optimization of these parameters gives a possibility to find the best conditions for electrochemical quantitive analysis of silicate and phosphate. This optimization was done before [9-11] and it was found that the best pH to form the silicomolybdate complex is equal to 1.4, whereas to form the phosphomolybdate complex it is necessary to acidify the solution to pH 1.0. To achieve appropriate pH, the oxidation time of molybdenum has to be conducted during 240s and 600s, respectively. Additionally, the formation of silicomolybdate complex takes about 5 min, whereas formation of phosphomolybdate complex 1 min only.

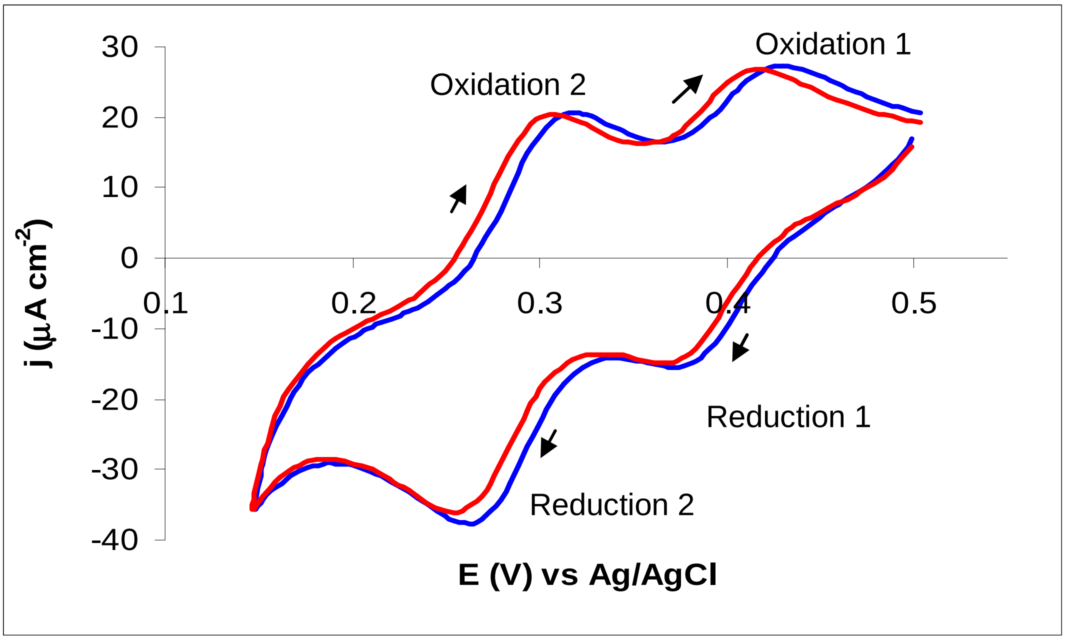

Figure 10a. Cyclic voltammograms recorded on a gold disk electrode (3 mm, 50 mV s^{-1}) for silicomolybdate complex (100 μmol L^{-1}) created by: (blue line) simple addition of sulphuric acid and sodium molybdate (VI) (pH 1.42, $[MoO_4^{2-}]$ =6.83 mmol L^{-1}); (red line) oxidation of molybdenum at constant current of 50 mA during 240s.

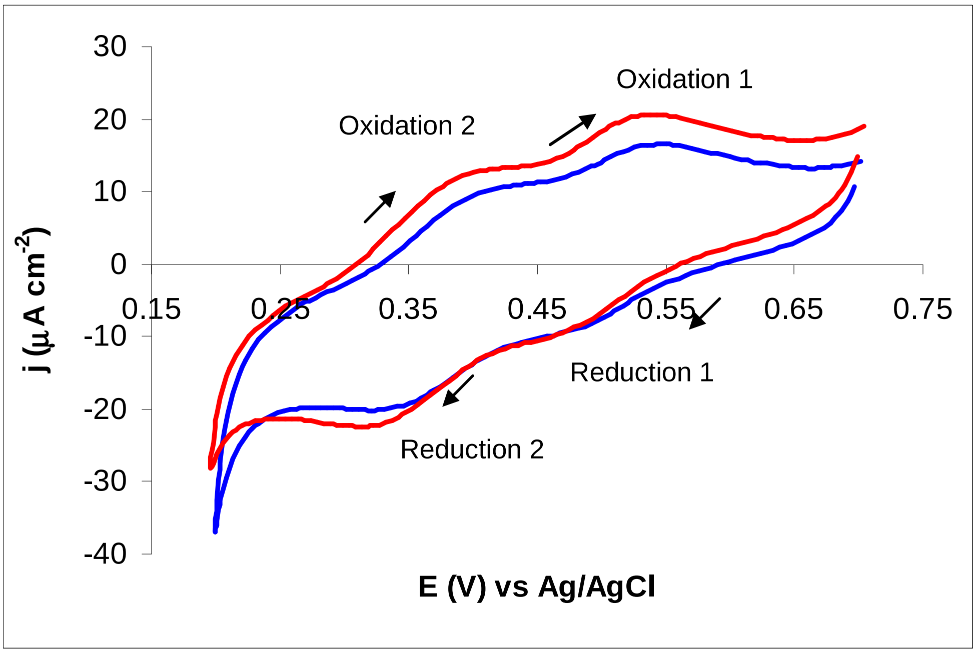

Figure 10b. Cyclic voltammograms recorded on a gold disk electrode (3 mm, 50 mV s^{-1}) for phosphomolybdate complex (100 µmol L^{-1}) created by: (blue line) simple addition of sulphuric acid and sodium molybdate (VI) (pH 1.0, $[MoO_4^{2-}]$=16.7 mmol L^{-1}); (red line) oxidation of molybdenum at constant current of 50 mA during 600s.

Cyclic voltammograms at different scan rates for both complexes are presented on Fig. 11. Since the voltammograms for heteropolyoxomolybdates created by both methods are very similar, only those created by oxidation of molybdenum in the sample containing phosphate or silicate are presented. The results show that the peak potential is not dependent on scan rate whereas the peak current density (j_p) is proportional to the square root of scan rate ($\upsilon^{-1/2}$) and the oxidation peaks are as well pronounced as the reduction ones. These results are clearly indicative of a reversible mass-transport limited system. For clarity the slopes $j_p=f(\upsilon^{-1/2})$ are gathered in Table 2.

Table 2. Peak current density vs. square root of the scan rate, $j_p=f(\upsilon^{-1/2})$ for silicomolybdate and phosphomolybdate complexes created by both methods.

Peak	Phosphomolybdate complex created by :	Silicomolybdate complex created by :
simple addition of sulphuric acid and sodium molybdate		
Oxidation 1	$j_p=16.4\upsilon^{-1/2} + 5.90$, $R^2=0.978$	$j_p=32.2\upsilon^{-1/2} + 4.59$, $R^2=0.982$
Oxidation 2	$j_p=56.3\upsilon^{-1/2} – 2.68$, $R^2=0.996$	$j_p=81.2\upsilon^{-1/2} + 2.55$, $R^2=0.994$
Reduction 1	$j_p=-32.6\upsilon^{-1/2} – 2.95$, $R^2=0.998$	$j_p=-49.3\upsilon^{-1/2} – 4.94$, $R^2=0.991$
Reduction 2	$j_p=-49.1\upsilon^{-1/2} + 1.46$, $R^2=0.997$	$j_p=-93.9\upsilon^{-1/2} + 7.08$, $R^2=0.993$
oxidation of molybdenum at constant current of 50 mA		
Oxidation 1	$j_p=27.86\upsilon^{-1/2} + 6.57$, $R^2=0.987$	$j_p=37.6\upsilon^{-1/2} +3.36$, $R^2=0.972$
Oxidation 2	$j_p=65.3\upsilon^{-1/2} – 2.25$, $R^2=0.993$	$j_p=84.5\upsilon^{-1/2} +1.47$, $R^2=0.993$
Reduction 1	$j_p=-57.4\upsilon^{-1/2} + 2.82$, $R^2=0.998$	$j_p=-47.5\upsilon^{-1/2} – 4.96$, $R^2=0.996$
Reduction 2	$j_p=-43.1\upsilon^{-1/2} – 4.21$, $R^2=0.995$	$j_p=-94.2\upsilon^{-1/2} +5.35$, $R^2=0.999$

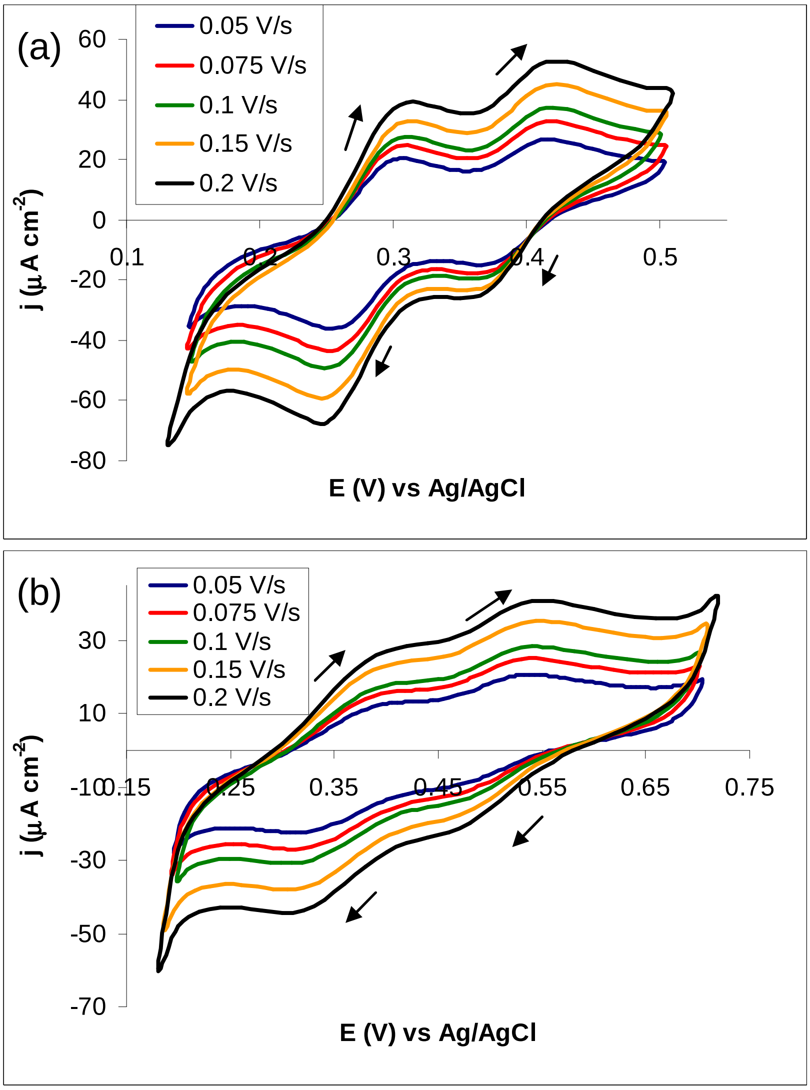

Figure 11. Cyclic voltammograms recorded on a gold disk electrode (3 mm) at different scan rates for 100 µmol L^{-1} of silicomolybdate complex (a) and phosphomolybdate (b) created by oxidation of molybdenum during 240 s (silicomolybdate complex) or 600 s (phosphomolybdate complex) at constant current of 50 mA.

4.3.2. Linear sweep voltammetry

Linear sweep voltammetry for heteropolyoxomolybdate was performed on a 3 mm rotating disk gold electrode (5 mV s^{-1}, 1000 rpm) after oxidation of molybdenum in 0.6 mol L^{-1} NaCl solution containing phosphate or silicate at a concentration of about 100 µmol L^{-1}. For comparison, a linear sweep voltammetry was made for heteropolyoxomolybdates created by addition of sodium molybdate (VI) and sulphuric acid to the 0.6 mol L^{-1} NaCl solution containing phosphate or silicate at a concentration of about 100 µmol L^{-1}, where the value of molybdate concentration and pH were the same as those achieved during oxidation of molybdenum. The resulting voltammograms are presented on Fig 12. The voltammograms for heteropolymolybdates created by oxidation of molybdenum were performed firstly from zero-current potential ($E_{I=0}$) to increasing potentials and then to decreasing ones. Finally, both curves were plotted on the same figure.

Linear sweep voltammetry for silico- and phosphomolybdate created by simple addition of acid and sodium molybdate (VI) to the sample containing phosphate or silicate was already done by Carpenter et al. [5]. Similar curves were achieved in this work and present two waves. It can be seen that the first wave shows reduction of complexes in a 2e$^-$ process followed by a further 3e$^-$ step. According to the results presented above we can propose the following electrode reduction reactions (7 a-d):

$$PMo_{12}O_{40}^{3-} + 2e^- + 2H^+ \leftrightarrow H_2PMo_2^{V}Mo_{10}^{VI}O_{40}^{3-} \quad (7a)$$

$$H_2PMo_2^{V}Mo_{10}^{VI}O_{40}^{3-} + 3e^- + 3H^+ \leftrightarrow H_5PMo_5^{V}Mo_7^{VI}O_{40}^{3-} \quad (7b)$$

$$SiMo_{12}O_{40}^{4-} + 2e^- + 2H^+ \leftrightarrow H_2SiMo_2^{V}Mo_{10}^{VI}O_{40}^{4-} \quad (7c)$$

$$H_2SiMo_2^{V}Mo_{10}^{VI}O_{40}^{4-} + 3e^- + 3H^+ \leftrightarrow H_5SiMo_5^{V}Mo_7^{VI}O_{40}^{4-} \quad (7d)$$

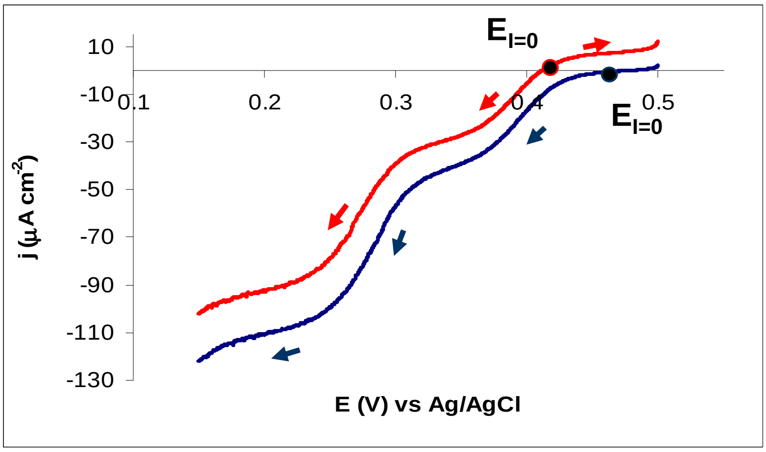

Figure 12a. Linear sweep voltammograms recorded on a rotating gold disk electrode (3 mm, 5 mV s^{-1}, 1000 rpm) for silicomolybdate complex (100 μmol L^{-1}) created by: (blue line) simple addition of sulphuric acid and sodium molybdate (VI) (pH 1.42, [MoO_4^{2-}]=6.83 mmol L^{-1}); (red line) oxidation of molybdenum at constant current of 50 mA for 240s.

However, linear sweep voltammograms for heteropolyoxomolybdates created by oxidation of molybdenum differ from those achieved by simple addition of sulphuric acid and sodium molybdate (VI) to the sample containing phosphate or silicate. Voltammograms for heteropolyoxomolybdates formed by oxidation of molybdenum show an oxidation wave which is not present on voltammograms for heteropolyoxomolybdates formed by simple addition of sodium molybdate and sulphuric acid. Besides, the zero current potential ($E_{I=0}$) reaches a constant value a long time after immersing the electrode and is shifted toward less positive potentials. These results suggest that during oxidation of molybdenum mixed valence heteropolyoxomolybdates (V, VI) are formed. Moreover, the ratio of current density of oxidation over current density of reduction waves gives a possibility to calculate the percentage content of Mo(V) and Mo(VI). The oxidation wave represents the oxidation of Mo(V) to (VI) and the reduction wave the reduction of Mo(VI) to Mo(V). Presuming that the only form of heteropolymolybdate species formed in this work is Keggin anion, the proposed forms of silicomolybdate are: $Si(Mo_2{}^{V}Mo_{10}{}^{VI}O_{40})^{4-}$ – 60% and $Si(Mo_3{}^{V}Mo_9{}^{VI}O_{40})^{4-}$ – 40% , whereas the main form of phosphomolybdate is $P(Mo_6{}^{V}Mo_6{}^{VI}O_{40})^{3-}$.

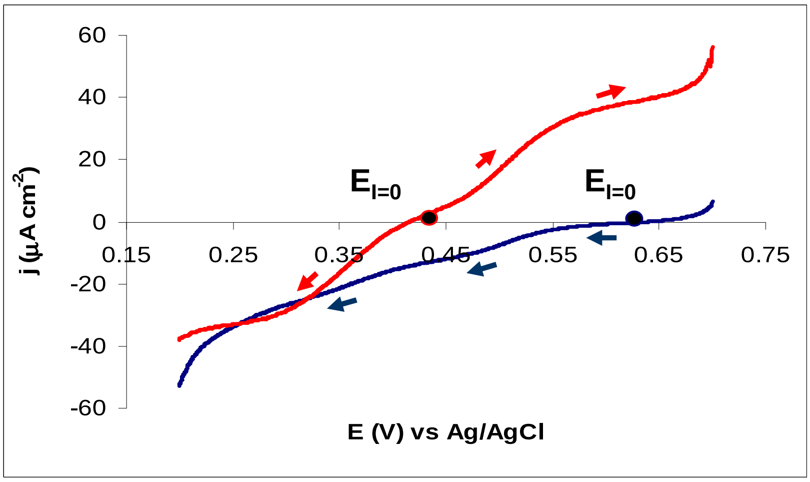

Figure 12b. Linear sweep voltammograms recorded on a rotating gold disk electrode (3 mm, 5 mV s^{-1}, 1000 rpm) for phosphomolybdate complex (100 µmol L^{-1}) created by: (blue line) simple addition of sulphuric acid and sodium molybdate (VI) (pH 1, $[MoO_4{}^{2-}]$=17.3 mmol L^{-1}); (red line) oxidation of molybdenum at constant current of 50 mA for 600s.

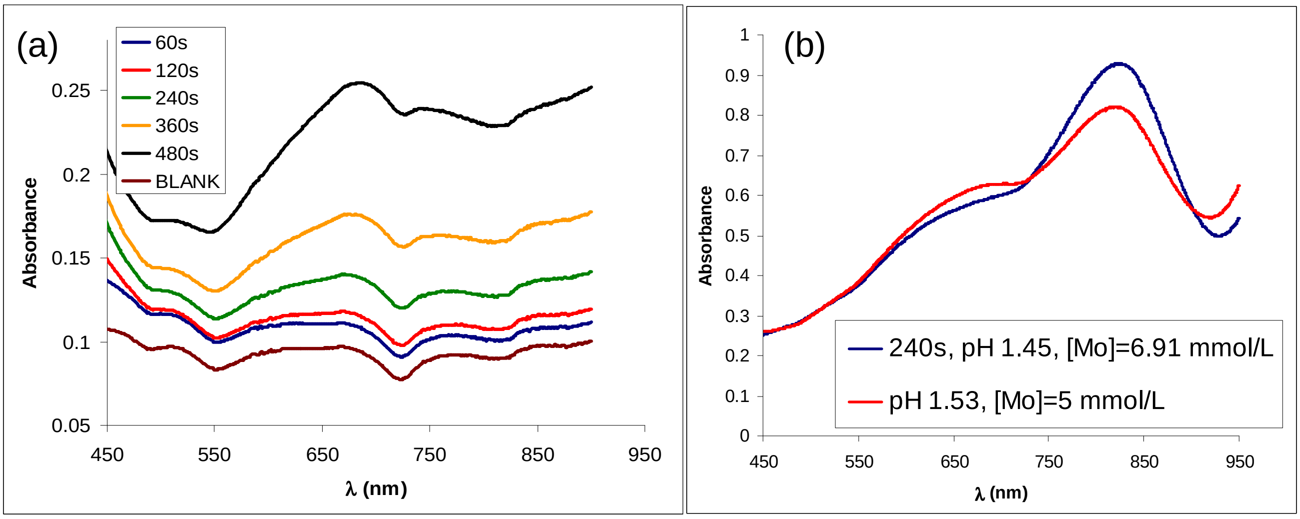

Figure 13. (a) Absorbance as a function of wavelength for molybdates created by oxidation of molybdenum in 0.6 mol L^{-1} NaCl solution containing silicate at concentration of 140 µM at constant current of 50 mA during different times. (b) Absorbance as a function of wavelength for molybdates created by both methods and treated by ascorbic acid.

The existence of mixed valence heteropolymolybdates can be confirmed by spectrophotometry. The data shows peaks at wavelengths corresponding to molybdenum blue spectrum with a maximum at 800 nm (Fig. 13a). This kind of spectrum did not appear if only Mo (VI) is present in the solution.

Moreover, addition of ascorbic acid after the oxidation of molybdenum increases the absorbance value and the shape of the spectrograms remains typical of those obtained by simple addition of sodium molybdate and sulphuric acid to the sample containing phosphate or silicate (Fig. 13b).

Linear sweep voltammograms registered at different rotation rates for both complexes formed by both methods are presented on Fig 14. The results show that the potential half wave (E_p) is not dependent on rotation rate whereas current density (j_{lim}) is proportional to the square root of rotation rate ($\omega^{-1/2}$). This characteristic indicates a mass-transport controlled system. For clarity the plots (j_{lim})=f($\omega^{-1/2}$) are gathered in Table 3

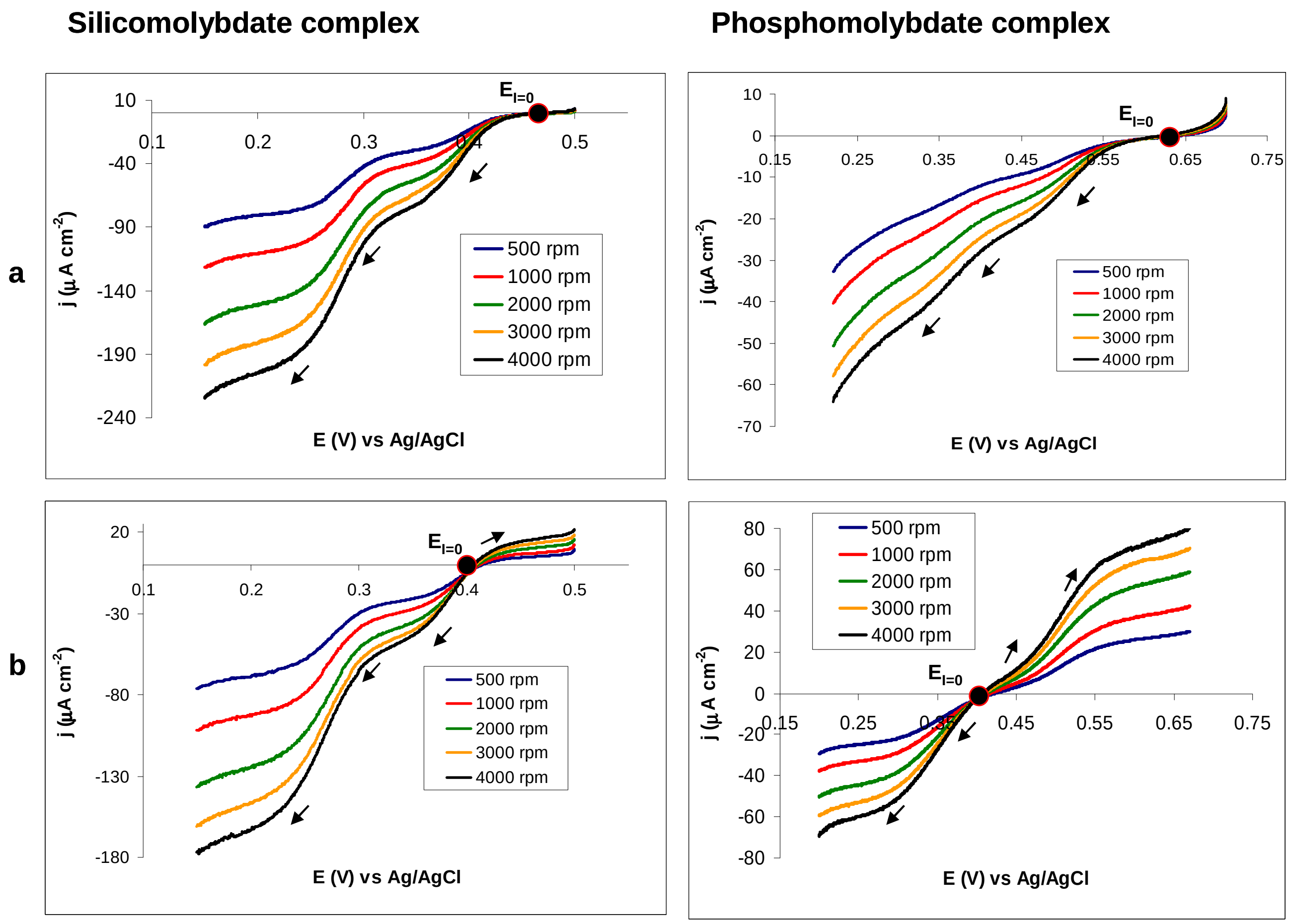

Silicomolybdate complex

Phosphomolybdate complex

Figure 14. Linear sweep voltammogram recorded on a rotating gold disk electrode (3 mm, 5 mV s^{-1}) at different rotation rates for 100 µmol L^{-1} of silicomolybdate complex (left insets) and phosphomolybdate (right insets) created by: (a) simple addition of sulphuric acid and sodium molybdate (VI) [for silicomolybdate complex: pH 1.42, MoO_4^{2-} = 6.83 mmol L^{-1}; for phosphomolybdate complex: pH 1, MoO_4^{2-} = 16.7 mmol L^{-1}]; (b) oxidation of molybdenum during 240 s (silicomolybdate complex) or 600 s (phosphomolybdate complex) at constant current of 50 mA.

Table 3. Limiting current density vs. square root of rotation rate, $j_{lim}=f(\omega^{-1/2})$ for silicomolybdate and phosphomolybdate complexes created by both methods.

Wave	Phosphomolybdate complex created by :	Silicomolybdate complex created by :
a) simple addition of sulphuric acid and sodium molybdate		
Reduction 1	$j_{lim}=-0.61\omega^{-1/2}$ -7.16, $R^2=0.999$	$j_{lim}=-3.06\omega^{-1/2}$ -12, $R^2=0.999$
Reduction 2	$j_{lim}=-0.30\ \omega^{-1/2}$ – 2.56, $R^2=0.999$	$j_{lim}=-1.17\ \omega^{-1/2}$ – 5.61, $R^2=0.999$
b) oxidation of molybdenum at constant current of 50 mA		
Oxidation	$j_{lim}=1.11\ \omega^{-1/2}$ +1.52, $R^2=0.999$	$j_{lim}=0.27\ \omega^{-1/2}$ -0.85, $R^2=0.997$
Reduction 1	$j_{lim}=-0.86\ \omega^{-1/2}$ – 6.02, $R^2=0.999$	$j_{lim}=-2.32\ \omega^{-1/2}$ -18.9, $R^2=0.997$
Reduction 2	-	$j_{lim}=-0.67\ \omega^{-1/2}$ – 8.55, $R^2=0.995$

The linear sweep voltammograms for the reduction of the phosphomolybdate species differ from those of the silicomolybdate complex. The waves are not as well formed; they are less steep and they overlap to a greater extent. The limiting currents densities for the phosphomolybdate complex are lower than for the silicomolybdate one. They are not proportional to the radii of the microdisks, being less than the expected ones. These results confirm that the electrode reactions are preceded by a reaction of protonation; this chemical step is faster for the silicomolybdate than for phosphomolybdate complex.

5. CONCLUSION

The purpose of this work was to unravel which kinds of molybdates are formed during anodic oxidation of molybdenum in seawater. The molybdenum oxidation in seawater and in 0.6 mol L^{-1} NaCl solution show similar behaviour as demonstrated by calculations from Tafel plot slopes where the determined anodic transfer coefficient and exchange current density were almost identical for both solutions and equal to about 0.46 and 10^{-4}, respectively.

Electrochemical behaviour of isopoly- and heteropolyoxomolybdates was investigated. The complexes were formed by two methods: one based on oxidation of molybdenum in artificial seawater and the second based on classical addition of sulphuric acid and sodium molybdate which served as a reference method. The investigation shows that the isopolyoxomolybdates formed by oxidation of molybdenum differs from those created by simple addition of reagents. However, it seems that the heteropolyoxomolybdates created by both methods have similar forms. Additionally, the results supported by spectrophotometry indicate formation of mixed valence molybdates (V/VI) during molybdenum oxidation in seawater in presence and absence of phosphate or silicate.

The formed isopolyoxomolybdate shows complicated electrode reactions. Cyclic voltammograms clearly indicate a mass-transport controlled quasi-reversible system, but the linear sweep voltammetry uncovers also the adsorption of reduced species and a kinetically limited reaction. The electrochemical behaviour of molybdate complexes change if phosphate or silicate is present in the solution. The cyclic voltammograms represent a typical reversible mass-transport controlled system with coupled homogeneous reaction, probably protonation, which prevents rapid electron transfer and influences current magnitude. The protonation step is slower for phosphomolybdate complex and it has greater influence on voltammograms. The cyclic voltammograms for phosphomolybdate species show peaks which are not as well formed as those for silicomolybdate complex. The peaks separation (E_{pa}-E_{pc}) is bigger on the phosphomolybdate voltammograms (80 mV) than for silicomolybdate ones (60 mV). Finally, the peak currents densities for the phosphomolybdate complex are lower than for the silicomolybdate. These results explain how delicate the problem of phosphate detection by electrochemistry is. The problem intensifies at low phosphate concentrations (which is the case in the seawater) since complicated electrode reactions coupled with high capacity current lead to disappearance of the characteristic reduction and oxidation peaks [11] and thus, the detection of phosphate by cyclic voltammetry is very difficult.

ACKNOWLEDGMENTS

We are grateful to the GET (Géoscience Environment Toulouse) laboratory (Toulouse, France) for access to a spectrophotometer. Justyna Jońca is supported by a Marie Curie PhD grant within SENSEnet ITN (EC Framework Programme 7, grant agreement No 237868). William Giraud is supported by the Foundation STAE (Sciences and Technologies for Space and Aeronautics) within the project ‘‘MAISOE’’ (Microlaboratories of *in situ* Analyses for Environmental Observatories).

References

1. W. V. Truesdale, J. S. Smith, *Analyst*, 101 (1976) 19.
2. L. I. Gordon, J. C. Jennings, A. A. Ross, J. M. Krest, WOCE, Method Manual. W. H. P. Office Report (1993) 68.
3. D. Thouron, R. Vuillemin, X. Philippon, A. Laurenço, C. Provost, A. Gruzado, V. Garçon, *Anal. Chem.*, 75, (2003) 2601.
4. A. G. Fogg, N. K. Bsebsu, *Analyst* 106 (1981) 1288.
5. N. Carpenter, A. W. E. Hodgson, D. Pletcher, *Electroanalysis* 9 (1997) 1311.
6. L. Guanghan, W. Xiaogang, L. Yanhua, Y. Shenlai, *Talanta* 49 (1999) 511.
7. S. M. Harden, W. K. Nonidez, *Anal. Chem.* 56 (1984) 2218.
8. J. C. Quintana, L. Idrissi, G. Palleschi, P. Albertano, A. Amine, M. El Rhazi, D. Moscone, *Talanta* 63 (2004) 567.
9. M. Lacombe, V. Garçon, M. Comtat, L. Oriol, J. Sudre, D. Thouron, N. Le Bris, C. Provost, *Mar. Chem.* 106 (2007) 489.
10. M. Lacombe, V. Garçon, D. Thouron, N. Le Bris, M. Comtat, 2008. *Talanta* 77 (2008) 744.
11. J. Jońca, V. León- Fernàndez, D. Thouron, A. Paulmier, M Graco, V. Garçon, *Talanta* 87 (2011) 161.
12. M. Koening, H. Goehr, *Ber. Bunsenges. Phys. Chem.*, 67 (1963) 837.
13. M. Itagaki, T. Suzuki, K. Watanabe, *Electrochim. Acta*, 42 (1997) 1081.
14. M. Bojinov, I. Betova, R. Raicheff, *J. Electroanal. Chem.* 381 (1995) 123.
15. M. Bojinov, I. Betova, R. Raicheff, *Electrochim. Acta*, 41 (1996) 1173.
16. M. N. Hull, *J. Electroanal. Chem.*, 38 (1972) 143.
17. T. V. Chukalovskaya, N. D. Tomashov, V. D. Manaskaya, *Zashchita Metallov* 20 (1984) 864.
18. K. Wang, Y.-S. Li, P. He, *Electrochim. Acta* 43 (1998) 2459.
19. R. D. Armstrong, M. F. Bell, A. A. Metcalfe, *J. Electroanal. Chem.*, 84 (1977) 62.
20. S. Himeno, N. Niiya, T. Ueda, *Bull. Chem. Soc. Jpn.* 70 (1997) 631.

21. C. V. Krishnan, M. Garnett, B. Hsiao, B. Chu, *Int. J. Electrochem. Sci*. 2 (2007) 29.
22. K. H. Tytko, B. Schonfeld, B. Buss, O. Glemnser, *Angew. Chem. Int. Ed*., 12 (1973) 330.
23. P. Chalilopyil, F. C. Anson, *Inorg. Chem.*, 17 (1978) 2418.
24. A. K. Pettersson, B. Karlberg, *Anal. Chim. Acta* 378 (1999) 183.
25. M. T. Pope (1983) *Heteropoly and Isopoly Oxometalates,* Springer-Verlag, New York.
26. C. E. Easterly, D. M. Hercules, M. Houalla, *Applied Spectroscopy* 55 (2001) 1671.
27. J. J. Cruywagen, A. G. Draaijer, J. B. B. Heyns, E. A. Rohwer, *Inorg. Chim. Acta* 331 (2002) 322.
28. V. V. Kuzenstov, M. R. Pavlov, D. I. Zimakov, S. A. Chepeleva, V. N. Kudryavtsev, *Rus. J. Electrochem*., 40 (2004) 711.
29. A. J. Bard and L. R. Faulkner: *Electrochemical methods: Foundamentals and applications"*, John Wiley and Sons, INC. (2001), New York, 341.